A hybrid frequency-time domain technique for ground effect identification

A. Vitale, N. Genito, L. Garbarino, U. Ciniglio and F. Corraro
a.vitale@cira.it
CIRA, Italian Aerospace Research Centre
Capua, Italy

ABSTRACT

The estimation from flight data of aerodynamic parameters for vehicle in steady-state conditions, perturbed by an identification manoeuvre, is a well-established technology, whereas system identification from dynamic flight data is a subject of continuous interest. This paper presents a hybrid frequency and time domain technique for identification of vehicle longitudinal aerodynamic model, including the ground effect. Identification is performed in the framework of a multi-step approach, in which, first aerodynamic coefficients are estimated in the frequency domain, using an equation error method; then time domain techniques are applied to identify out of ground effect aerodynamic derivatives and ground effect model parameters. The technique was successfully applied to flight data of an experimental ultra light aircraft. Identification results showed that the proposed method works properly also in the dynamic phases of the flight or when no dedicated identification manoeuvres are executed. Moreover, the identified longitudinal aerodynamic model was used to design the flight control system that successfully performed many autonomous landings.

NOMENCLATURE

a_i, b_i, c_i	ground effect model's parameters
b, c	wing span [m] and aerodynamic chord [m]
C	vector of aerodynamic non dimensional force and moment coefficients
C_L, C_D	longitudinal non dimensional aerodynamic force coefficients, referred to stability axes
C_{Li},D_{Li},C_{Mi}	derivatives of the aerodynamic coefficients with respect to variable i
C_m	non dimensional aerodynamic pitching moment coefficient
C_X, C_Z	longitudinal non dimensional aerodynamic force coefficients, referred to body axes
C_T	thrust coefficient
De	propeller diameter [m]
g	gravity acceleration [m/s^2]
G, F	gradient and Hessian of the cost function
h	height above ground level [m]
h_{GE}	non dimensional height above ground level above which ground effect is negligible
I_y	pitching moment of inertia [kg*m^2]
j	imaginary unit
J	cost function to be optimised
K_D	induced drag factor
l_t	distance between vehicle gravity centre and tail aerodynamic centre [m]
m	mass [kg]
M	number of windows used to estimate aerodynamic coefficients
N	number of measurement samplings
q	pitch rate referred to aircraft axis [deg/s]
$\bar{q}$	dynamic pressure [Pa]
R	measurement noise covariance matrix
S	aerodynamic reference surface [m^2]
T	thrust [N]
u, w	longitudinal velocity components referred to aircraft axes [m/s]
U	vehicle input vector
V	true air speed [m/s]
x	vehicle state vector

Paper No. 3471. Manuscript received 25 June 2009, revised 17 November 2009 accepted 8 January 2010.

https://doi.org/10.1017/S0001924000003833 Published online by Cambridge University Press

$X(j\omega)$	Fourier transform of $x(t)$
x_{gc}	X-axis co-ordinate of the gravity centre, in percentage of aerodynamic chord
X_{NP}	X-axis co-ordinate of the neutral point, in percentage of aerodynamic chord
$\mathbf{y}$	output vector of the simulation model
$\mathbf{z}$	flight measurement vector
α	angle-of-attack [deg]
γ	advance ratio
δ_F	normalised flap deflection
δ_S	stabilator deflection [deg]
Δt	time sampling interval [s]
$\Delta C_{i\text{-}GE}$	variation of non dimensional aerodynamic coefficient C_i due to ground effect
θ	pitch angle [deg]
$\boldsymbol{\lambda}$	vector of unknown aerodynamic derivatives
ρ	air density [kg/m^3]
ω	pulsation [rad/s]
ω_e	propeller angular velocity [deg/s]
F	subscript to denote flap configuration
GE	subscript to denote values in ground effect
OGE	subscript to denote values out of ground effect
$\hat{}$	superscript to denote estimated values

1.0 INTRODUCTION

The estimation from flight data of stability and control aerodynamic derivatives for vehicle in steady-state conditions perturbed by an identification manoeuvre is a well-established technology[1,2], whereas system identification from dynamic flight data (such as during take-off and landing) is a subject of continuous interest[2-6].

Aerodynamic characteristics of an aircraft can change in proximity of the ground. Usually, ground effect on stability and control derivatives is of less importance and it is easily compensated for by piloting technique. On the other hand, automatic landing system requires high fidelity simulation model. Then, in order to develop autonomous vehicle, it is necessary a better understanding of the ground effect.

Many studies are reported in the literature on this topic. Although clearly documented, a satisfactory physical explanation for the dynamic effects has not been proven. Ground effect prediction has been performed by using analytical methods[7] and wind tunnel tests[8]. Both these approaches have had few opportunities for in flight validation. In fact, it is difficult to get adequate dynamic experimental data in order to carry out ground effect estimation from flight measurements. Moreover, they often simulate ground effect in steady-state conditions (constant height above ground level), which could be rather different from ground effect in dynamic conditions[9] (such as landing approaches).

This paper presents a hybrid frequency and time domain method for identification of longitudinal aerodynamic model from flight data. Identification is performed in the framework of a multi-step strategy, which decomposes the complex starting problem in simplified sub-problems. First identification step is carried out in the frequency domain and it is aimed at estimating the global longitudinal aerodynamic coefficients. Next, time domain techniques are used to identify the longitudinal aerodynamic derivatives and the ground effect model.

The multi-step identification approach, which first performs the estimation of the global aerodynamic coefficients and next evaluates the model's parameters, was already successfully applied, both for in-flight aerodynamic derivatives estimation[10,11] and for ground effect evaluation during take off and landing[2-4]. Several techniques are proposed in the literature for the identification of the global aerodynamic coefficients. For what concerns in-flight applications, filtering techniques based on Kalman filter are used. These methods provide very accurate results, inclusive of consistent evaluation of the estimation uncertainty[11], but they require the tuning of the filter parameters, that is, process and measurement noise covariance matrices, in order to avoid convergence problems[10]. Furthermore, the dynamical behaviour of the unknowns (the global aerodynamic coefficients) should be modelled. To this end, stochastic processes are adopted, such as Gauss-Markov process[11], which should be characterised and tuned, too. On the other hand, the global aerodynamic coefficients needed for the identification of ground effect model are computed from flight measurements and vehicle inertial data, by using static algebraic relations and without performing any estimation[2-4]. This approach permits to easily compute the aerodynamic coefficients, but their evaluations are affected by measurement errors.

The frequency domain technique proposed in this paper for the estimation of the aerodynamic coefficients (both in-flight and during landing) is a compromise between simplicity and accuracy of the estimation. In fact it doesn't require any cumbersome tuning process or model definition, neither it presents convergence problems. Furthermore, since the technique is equivalent to a low-pass filter, it allows filtering out all the high frequency measurement noises.

In the proposed strategy, the estimation of aerodynamic derivatives is performed in the second identification step through the maximum likelihood methodology, because it represents a well assessed technique for the evaluation of constant parameters[2,12]. Moreover, the application of a bounded-variable optimisation method allows exploiting all the available a priori information on the unknown parameters (such as bounds on the unknowns).

Finally, the multi-step approach, denoted in the literature as estimation before modelling[10], is well suited for the identification of the ground effect, which is usually modelled as an incremental variation with respect to the baseline aerodynamic model estimated out of ground effect[2-4]. In fact, the multi-step strategy allows estimating first the global variation due to the ground effect. Next, the ground effect is modelled and the related parameters are estimated. The global coefficient variation can be computed without exciting the vehicle dynamics, because it is simply due to the ground proximity. For that reason, this procedure works properly also during critical flight phases, such as in ground proximity, where no identification manoeuvres can be performed and it is the main advantage of the technique.

The proposed method was applied to flight data of an experimental ultra light aircraft, in order to estimate stability and control aerodynamic derivatives out of ground effect and ground effect parameters. The identified longitudinal aerodynamic model, inclusive of ground effect, was used to design the vehicle flight control system, that successfully performed many autonomous landings[13].

The present work was carried out in the framework of the Italian funded project TECVOL, executed by the CIRA (Italian Aerospace Research Centre), with the aim of developing innovative technologies for flight autonomy and collision avoidance.

2.0 VEHICLE DESCRIPTION

The technologies developed in the CIRA TECVOL project are deployed by means of a flying test bed consisting of a piloted aircraft equipped with on-board avionics system and on-ground control station designed and integrated by CIRA. It is able to allow experimentation about autonomous take-off and landing, mission automation and detect, sense and avoid. The flying platform, shown in Fig. 1, is an experimental ultra light aircraft with designed empty weight of 281kg, max take-off weight of 450kg, max speed s/l about 218km/h, cruising speed about 190km/h, wing area of 13·2m^2, wing span of 9·6m and maximum engine power of 100hp.

The vehicle's aerodynamic effectors are stabilator, ailerons and rudder, for longitudinal, lateral and directional control, respectively. Moreover a plain flap is used to increase lift during take-off and

https://doi.org/10.1017/S0001924000003833 Published online by Cambridge University Press

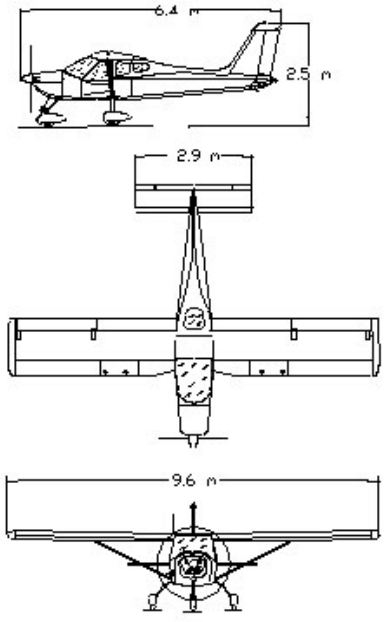


Figure 1. Aircraft 3-view.

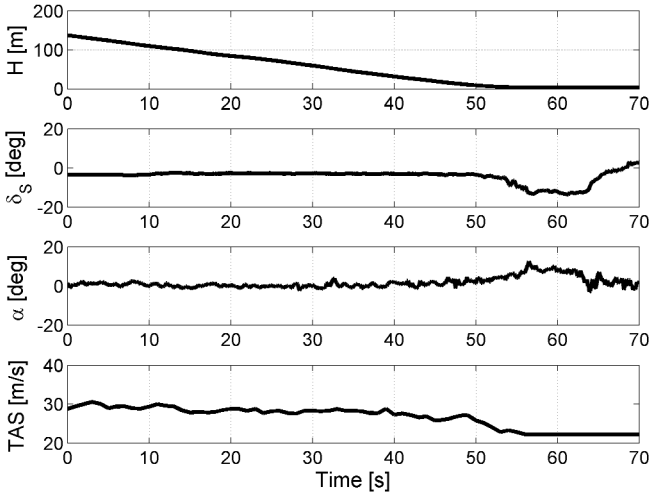


Figure 2. Landing manoeuvre.

landing. Wind-tunnel tests and semi-empirical methods were used to compute a pre-flight aerodynamic model, which was the most reliable information on the vehicle aerodynamics before performing system identification from flight data. It is worthy to note that the pre-flight aerodynamic model and the one estimated from flight data have the same structure.

On board avionics system includes all devices needed to perform the in flight experimental validation of advanced guidance, navigation and control functionalities. The devices were selected among the commercial-off-the-shelf (COTS) ones, and they include: the flight control computer (FCC), the navigation sensor suite, a radar device, the digital electromechanical servos, and a digital bidirectional data link.

The FCC is an embedded real-time computer based on a PowerPC processor, provided by the supplier with a tool based on the most advanced control system rapid prototyping methodologies. This software environment enables the automatic coding of the real-time software directly from MATLAB/SIMULINKTM diagrams, thus being extremely efficient from data acquisition and algorithm in-flight testing point of view.

The Navigation sensor suite includes:

- two differential GPS, one in code differential mode and one in RTK (real-time kinematic) L1/L2 mode, capable to provide position measurements with an accuracy of few centimetres;
- solid state attitude heading reference system (AHRS), used to measure body axis accelerations, Euler angles and angular rates;
- two dedicated sensors for height above ground level measurements, respectively using radar and laser technology (only one altimeter sensor can be mounted because of weight limitations);
- air data computer (ADC) with a dedicated air data probe capable to provide indicated air speed (IAS), true air speed (TAS), barometric pressure, aerodynamic angles.

A radar device is installed on the top of the plane, in order to detect other planes presence.

The digital electromechanical servos are used to command both aerodynamic surfaces and throttle, driven by the FCC.

Finally, the digital bidirectional data link system allows exchanging data between on board FCC and the ground control station (GCS) with a maximum bit-rate of 9·600 bit/sec in uplink and 115·200 bit/sec in downlink up to about 6km of operative range.

The GCS is installed in a big shelter fixed on the ground near the runway. It is designed to show telemetry data and to present it to the flight test engineers through dedicated human machine interfaces (HMI). It can be used also for remote reconfiguration of the on board avionics system. Its main features are:

- bidirectional data link with a range of about 6km
- GPS base station used to send the differential correction to the on board GPS
- meteorological station
- virtual cockpit HMI
- engineering HMI
- automatic collision avoidance HMI

3.0 FLIGHT TESTING

Flight data were gathered far from ground and in ground proximity, in order to estimate both out of ground effect longitudinal aerodynamic derivatives and ground effect parameters.

Flight data in ground proximity were acquired during the landing phase. An example of landing manoeuvre is presented in Fig. 2. These data were also used to design the autonomous landing system.

Flight test manoeuvres were performed to estimate the aerodynamic derivatives out of ground effect. They were designed in order to excite the aircraft longitudinal modes. Two type of stabilator manoeuvres were selected: doublet and 3-2-1-1. A 3-2-1-1 manoeuvre executed in flight is shown in Fig. 3. The intensity and step period of the identification manoeuvres were tuned performing sensitivity analysis, based on Cramer Rao Bound computation[2], on the aerodynamic parameters of interest. To this end, simulated data were generated using the pre-flight aerodynamic model.

In order to perform system identification, flight measurements of acceleration, velocity, height above ground level, angular rates, attitude, aerodynamic effectors, thrust, and aerodynamic angles were collected at the sampling rate of 10Hz.

https://doi.org/10.1017/S0001924000003833 Published online by Cambridge University Press

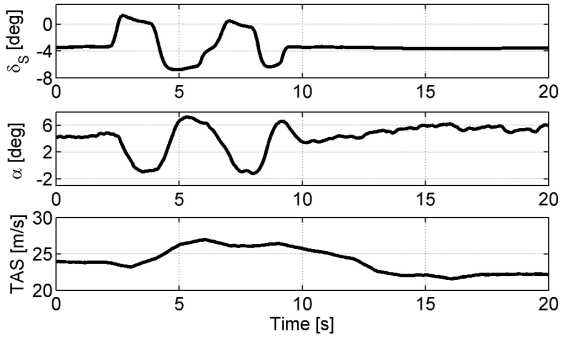


Figure 3. Flight test: 3-2-1-1 manoeuvre.

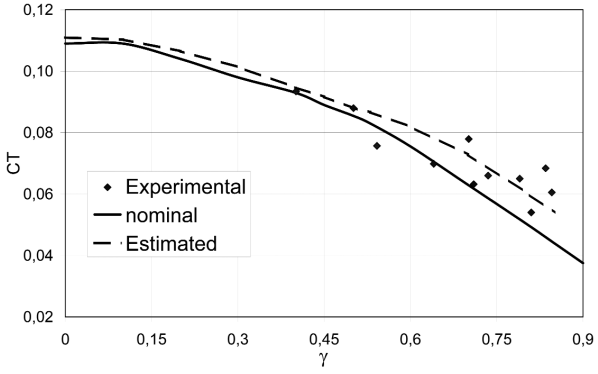


Figure 4. Nominal and identified thrust coefficient.

4.0 VEHICLE'S MODEL

The present section describes the model used to perform system identification from flight data. This model is composed of the aircraft dynamic equations, the aerodynamic model (including ground effect) and the thrust model.

In the hypothesis of symmetric aircraft about its longitudinal plane and assuming to fly at small sideslip angle, we can use the simplification of uncoupled longitudinal and lateral-directional dynamic equations. It is also assumed that the thrust T is aligned to the vehicle longitudinal X-axis. Then, the longitudinal dynamic behaviour of the vehicle is described in body axes by the following equations

$$(\dot{u}+qw)m=\bar{q}SC_X-\mathrm{g}\,\mathrm{Sin}\vartheta+T \quad \ldots(1)$$

$$(\dot{w}-qu)m=\bar{q}SC_Z+g\,\mathrm{Cos}\vartheta \quad \ldots(2)$$

$$\dot{q}I_Y=\bar{q}ScC_m \quad \ldots(3)$$

$$\dot{\vartheta}=q \quad \ldots(4)$$

Out of ground effect, the longitudinal aerodynamic model, in stability axes, is

$$\begin{aligned}C_L&=C_{L0}+C_{L0F}\delta_F+(C_{L\alpha}+C_{L\alpha F}\delta_F)\alpha+\\&+(C_{L\dot{\alpha}}+C_{L\dot{\alpha}F}\delta_F)\frac{\dot{\alpha}\,\mathrm{c}}{2V}+(C_{Lq}+C_{LqF}\delta_F)\frac{qc}{2V}+\\&+(C_{L\delta s}+C_{L\delta sF}\delta_F)\delta_s\end{aligned} \quad \ldots(5)$$

$$\begin{aligned}C_D&=C_{D0}+C_{D0F}\delta_F+(K_D+K_{DF}\delta_F)[C_{L0}+\\&+C_{L0F}\delta_F+(C_{L\alpha}+C_{L\alpha F}\delta_F)\alpha]^2\end{aligned} \quad \ldots(6)$$

$$\begin{aligned}C_m&=C_{m0}+C_{m0F}\delta_F-(X_{NP}+X_{NPF}\delta_F+\\&-x_{gc})(C_{L\alpha}+C_{L\alpha F}\delta_F)\alpha-\frac{\mathrm{l}_t}{c}[(C_{L\dot{\alpha}}+\\&+C_{L\dot{\alpha}F}\delta_F)\frac{\dot{\alpha}\,\mathrm{c}}{2V}+(C_{Lq}+C_{LqF}\delta_F)\frac{q\,\mathrm{c}}{2V}+\\&+(C_{L\delta s}+C_{L\delta sF}\delta_F)\delta_s]\end{aligned} \quad \ldots(7)$$

In Equations (5) to (7), the aerodynamic coefficients depend also on flap position. This dependence is linearly modelled through the non-dimensional coefficient δ_F which varies between 0 (no flap deflection) and 1 (maximum flap deflection, 36 degrees). Each aerodynamic derivative is composed of the contribution without flap and the flap contribution (denoted by subscript F). Both configurations, with and without flap deflection, are identified from flight data.

In order to reduce unknown parameters' number and to get a better estimation, the following relations between lift and pitching moment derivatives are introduced

$$C_{L\delta s}=-C_{m\delta s}\frac{c}{l_t}$$

$$C_{Lq}=-C_{mq}\frac{c}{l_t} \quad \ldots(8)$$

$$C_{L\dot{\alpha}}=-C_{m\dot{\alpha}}\frac{c}{l_t}$$

Ground effect appears when an aircraft flies in ground proximity. It can be modelled through non dimensional variations of the aerodynamic coefficients with respect to the values provided by Equations (5) to (7). We suppose that the variations have a parabolic dependence on the vehicle non dimensional height above ground level h/b. The variations are defined as

$$\Delta C_{iGE}=\begin{cases}0 & \text{if } h/b > h_{GE}\\ a_i\left(h/b\right)^2+b_i\left(h/b\right)+c_i & \text{otherwise}\end{cases} \quad \ldots(9)$$

where $i=\{L, D, m\}$ and a_i, b_i and c_i are the parameters that characterise the ground effect model. It is worthy to note that the aircraft experiments the maximum ground effect ΔC_{max} at touchdown (that is $h=0$). Moreover we assume that the variations and their derivatives with respect to h are continuous in $h/b = h_{GE}$. These assumptions mean that the parable in Equation (9) passes through the points $P_1 \equiv (0, \Delta C_{max})$ and $P_2 \equiv (h_{GE}, 0)$, and it has null tangent in P_2. These properties are used to identify the ground effect model as explained in Section 5.3.

Finally, the aerodynamic force coefficients in stability and body reference frames are related by

$$\begin{aligned}C_L&=-C_Z\mathrm{Cos}\alpha+C_X\mathrm{Sin}\alpha\\C_D&=-C_Z\mathrm{Sin}\alpha-C_X\mathrm{Cos}\alpha\end{aligned} \quad \ldots(10)$$

The model of the thrust is based on the Renard's[14] formula

$$T=C_T(\gamma)\rho D_e^4\left(\frac{\omega_e}{2\pi}\right)^2 \quad \ldots(11)$$

The nominal thrust coefficient curve $C_T(\gamma)$ was provided by the producer of the propeller and validated using experimental data gathered in dedicated flight tests. Since the nominal curve was shifted with respect to experimental C_T values, it was corrected performing estimation from flight data. The estimated curve was

https://doi.org/10.1017/S0001924000003833 Published online by Cambridge University Press

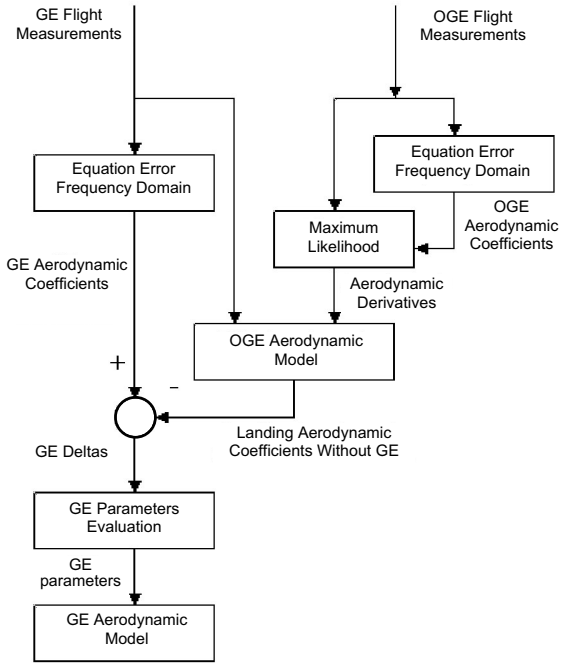


Figure 5. Flow-chart of the identification process.

obtained preserving the $C_T(\gamma)$ nominal shape, while fitting (in the least square sense) the experimental data. Nominal and estimated thrust coefficients are presented in Fig. 4, together with the experimental data. The difference between nominal and estimated curves is always lower than 20% and increases with respect to the advance ratio. It is worthy to note that prospective error on thrust coefficient estimation could have relevant effect only on the aerodynamic drag coefficient estimation, because the thrust is aligned to the vehicle longitudinal axis and the angle-of-attack experimented in flight is always small. Furthermore, since the ground effect analysis is determined primarily as the difference between in ground effect and out of ground effect conditions during landing approach, and since the thrust is held constant during the whole landing approach, small errors in the thrust estimate have negligible effect on ground effect model identification.

5.0 IDENTIFICATION METHODOLOGY

Two different problems are examined, that is, estimation of aircraft aerodynamic derivatives out of ground effect (OGE) and evaluation of ground effect (GE) characteristics.

First problem is solved in two steps, using an estimation before modelling approach[10]. In the first step a frequency domain equation error method[1] is applied to Equations (1) to (3), in order to estimate longitudinal aerodynamic coefficients (C_X, C_Z and C_m). Next, Equations (10) are used to compute aerodynamic coefficients in stability axes. Then estimation of stability and control derivatives (second step) is performed by means of maximum likelihood[2] methodology, based on bounded-variable Gauss-Newton optimisation method, applied to Equations (5) to (8).

First step described above is used to identify aerodynamic coefficients in ground effect, too. The comparison of so estimated coefficients and the analogous coefficients computed through aerodynamic model and aerodynamic derivatives estimated out of GE, allows to evaluate ground effect characteristics. The flow-chart of identification process is shown in Fig. 5 and detailed in the following sections.

5.1 Estimation of the aerodynamic coefficients

The estimation of the aerodynamic coefficients is carried out applying the Fourier Transform Regression technique[1] to Equations (1)-(3), rearranged in the following general form

$$\dot{\mathbf{x}} = \mathbf{f}(\mathbf{x},\mathbf{U},\mathbf{C}) = \mathbf{f}_1(\mathbf{x},\mathbf{U}) + \mathbf{f}_2(\mathbf{x})\mathbf{C} \qquad \ldots (12)$$

where

$$\mathbf{x} = [u, w, q, \vartheta]^T$$

$$\mathbf{U} = [T, \delta_S]$$

$$\mathbf{C} = [C_X, C_Z, C_m]^T$$

$$\mathbf{f}_1 = [-g\,\mathrm{Sin}\vartheta + T,\ g\,\mathrm{Cos}\vartheta,\ \bar{q}ScC_m,\ q]^T \qquad \ldots (13)$$

$$\mathbf{f}_2 = \begin{bmatrix} \bar{q}S & 0 & 0 & 0 \\ 0 & \bar{q}S & 0 & 0 \\ 0 & 0 & \bar{q}Sc & 0 \\ 0 & 0 & 0 & 0 \end{bmatrix}$$

and $\mathbf{x}$ and $\mathbf{U}$ are time dependent (time is dropped for the sake of simplicity).

Each aerodynamic coefficient belonging to the vector $\mathbf{C}$ depends on the vehicle state vector $\mathbf{x}$ and the stabilator deflection δ_S, included in the input vector. We suppose that in a small range of variations for $\mathbf{x}$ and δ_S, C can be approximated by a constant vector $\mathbf{C_i}$, equal to its mean value on the considered range, namely

$$\mathbf{C}(\mathbf{x},\delta_e) = \sum_{i=1}^{M} \mathbf{C}_i \Pi_i\left([\mathbf{x}_i, \mathbf{x}_{i+1}], [\delta_{si}, \delta_{si+1}]\right) \qquad \ldots (14)$$

where

$$\Pi_i\left([\mathbf{x}_i, \mathbf{x}_{i+1}], [\delta_{si}, \delta_{si+1}]\right) = \begin{cases} 1 & (\mathbf{x}, \delta_s) \in [\mathbf{x}_i, \mathbf{x}_{i+1}] \times [\delta_{si}, \delta_{si+1}] \\ 0 & \text{otherwise} \end{cases} \qquad \ldots (15)$$

Substituting Equation (14) in (12) and rearranging we get

$$\dot{\mathbf{x}} - \mathbf{f}_1(\mathbf{x},\mathbf{U}) = \sum_{i=1}^{M} \mathbf{f}_2(\mathbf{x})\mathbf{C}_i \Pi_i\left([\mathbf{x}_i, \mathbf{x}_{i+1}], [\delta_{si}, \delta_{si+1}]\right) = \sum_{i=1}^{M} \mathbf{f}_{2i}(\mathbf{x},\mathbf{U})\mathbf{C}_i \qquad \ldots (16)$$

It is worthy to note that $\mathbf{f_{2i}}$ is also function of δ_S, then it depends on the input U, too. We can evaluate the time histories of $\mathbf{f_1}$ and $\mathbf{f_{2i}}$ from flight measurements and consider $\mathbf{f_1}(t)$ and $\mathbf{f_{2i}}(t)$ as flight measurements themselves. The Fourier Transforms (FT) of $\mathbf{x}(t)$, $\mathbf{f_1}(t)$ and $\mathbf{f_{2i}}(t)$ are computed through[1]:

$$Z(j\omega) = \int_0^T z(t)\exp(-j\omega t)\,dt \approx \Delta t \sum_{i=0}^{N-1} z(t_i)\exp(-j\omega t_i) \qquad \ldots (17)$$

The Fourier Transform of $\dot{\mathbf{x}}$ is evaluated by means of Equation (17), if the measurement of $\dot{\mathbf{x}}$ is available. Otherwise it is get as the derivative of $\mathbf{X}(j\omega)$ in the frequency domain, that is FT($\dot{\mathbf{x}}(t)$) = $j\omega\mathbf{X}(j\omega)$. Finally, we can put Equation (16) in the Fourier domain in the form:

$$\mathbf{B}(j\omega) = \sum_{i=1}^{M} \mathbf{A}_i(j\omega)\mathbf{C}_i \qquad \ldots (18)$$

with $\mathbf{B}(j\omega)$ = FT($\dot{\mathbf{x}} - f_1(\mathbf{x},\mathbf{U})$), $\mathbf{A}_i(j\omega)$ = FT($f_{2i}(\mathbf{x},\mathbf{U})$). Equation (18) is evaluated for $L>M$ different values of ω. The L equations are then solved by means of least mean square technique, the $\mathbf{C_i}$ are estimated and the time history of $\mathbf{C}$ is determined interpolating the estimated values.

https://doi.org/10.1017/S0001924000003833 Published online by Cambridge University Press

5.2 Estimation of aerodynamic derivatives

The aerodynamic derivatives are estimated using a maximum likelihood methodology, based on bounded-variable Gauss-Newton optimisation method[2]. The model to be identified is defined by Equations (5)–(8). The vector of unknown parameters, denoted by λ, is composed of all the aerodynamic derivatives, with and without flap deflection, which are present in the model. The cost function optimised by the maximum likelihood technique is

$$J(\boldsymbol{\lambda},\mathbf{R}) = \frac{1}{2}\sum_{k=1}^{N}\left[\mathbf{z}(t_k)-\mathbf{y}(t_k)\right]^T \mathbf{R}^{-1}\left[\mathbf{z}(t_k)-\mathbf{y}(t_k)\right] + \\ + \frac{N}{2}\ln|\mathbf{R}| \qquad \ldots (19)$$

where t_k is the sampling time, $\mathbf{z}(t_k)$ is the measurement in t_k and $\mathbf{y}(t_k)$ is the system output vector, computed using simulation model and identified parameters.

Optimisation of J is carried out in two steps. In the first one it can be shown that, for any value of λ, the maximum likelihood estimate of $\mathbf{R}$ is given by

$$\hat{\mathbf{R}} = \frac{1}{N}\sum_{k=1}^{N}\left[\mathbf{z}(t_k)-\mathbf{y}(t_k)\right]\cdot\left[\mathbf{z}(t_k)-\mathbf{y}(t_k)\right]^T \qquad \ldots (20)$$

Then a constrained Gauss-Newton optimisation method is applied in order to update the parameter vector $\boldsymbol{\lambda}$. The linearly constrained optimisation problem, in which the constraints are simple bounds on the variables, is formulated as:

$$\min_{\boldsymbol{\lambda}} J(\boldsymbol{\lambda}) \qquad \text{with} \qquad \boldsymbol{\lambda}_{min} \le \boldsymbol{\lambda} \le \boldsymbol{\lambda}_{max} \qquad \ldots (21)$$

This problem is solved by means of the active set strategy proposed by Jategaonkar[2]. The parameters satisfying the constraints, denoted by subscript *free*, are iteratively updated, until convergence is reached, using the following relations

$$\boldsymbol{\lambda}_{free}^{i+1} = \boldsymbol{\lambda}_{free}^{i} + \Delta\boldsymbol{\lambda}_{free} \qquad \ldots (22)$$

$$\Delta\boldsymbol{\lambda}_{free} = -\mathbf{F}_{free}^{-1}\mathbf{G}_{free} \qquad \ldots (23)$$

$$\mathbf{F}_{free} = \frac{\partial^2 J}{\partial\boldsymbol{\lambda}_{free}^2} \approx \sum_{k=1}^{N}\left[\frac{\partial\mathbf{y}(t_k)}{\partial\boldsymbol{\lambda}_{free}}\right]^T \mathbf{R}^{-1}\left[\frac{\partial\mathbf{y}(t_k)}{\partial\boldsymbol{\lambda}_{free}}\right] \qquad \ldots (24)$$

$$\mathbf{G}_{free} = \frac{\partial J}{\partial\boldsymbol{\lambda}_{free}} = \sum_{k=1}^{N}\left[\frac{\partial\mathbf{y}(t_k)}{\partial\boldsymbol{\lambda}_{free}}\right]^T \mathbf{R}^{-1}\left[\mathbf{z}(t_k)-\mathbf{y}(t_k)\right] \qquad \ldots (25)$$

Parameters outside the allowable range, named constrained parameters, are set equal to the nearest allowable value (that is minimum or maximum bound).

The set of free parameters is updated after each iteration. If one of the parameters belonging to the free set hits the bounds, it is dropped from the free set and made constrained. On the other hand if the Kuhn–Tucker optimality conditions

$$\left(G_j < 0, \quad \text{for} \quad \lambda_j = \lambda_{j_max}\right) \text{ or } \left(G_j > 0, \quad \text{for} \quad \lambda_j = \lambda_{j_min}\right) \qquad \ldots (26)$$

are not satisfied for any of the constrained parameters, then those parameters are dropped from the constrained set and made free. In Equation (26) G_j, λ_j, λ_{j_min} and λ_{j_max} are the j-th component of the gradient G, the current estimation of the unknown vector, and its lower and upper bounds, respectively.

5.3 Evaluation of ground effect

The frequency domain equation error method, described in Section 5.1, is applied to estimate longitudinal aerodynamic coefficients in ground effect, too.

The global variations of the aerodynamic coefficients due to ground effect are evaluated by comparing the aerodynamic coefficients estimated from flight data gathered during landing with the analogous coefficients computed using landing flight data measurements and the aerodynamic model estimated out of ground effect, defined by Equations (5)–(7). More in detail, the variations are computed as[3]

$$\Delta C_{L-GE} = C_L - C_{L-OGE} - C_{L\alpha}\left(\alpha-\alpha_{OGE}\right) + \\ - C_{L\delta s}\left(\delta_s - \delta_{s-OGE}\right) \qquad \ldots (27)$$

$$\Delta C_{D-GE} = C_D - C_{D-OGE} - K_D\left[2C_{L0}C_{L\alpha}\left(\alpha + \right.\right. \\ \left.\left. -\alpha_{OGE}\right) + C_{L\alpha}^2\left(\alpha-\alpha_{OGE}\right)^2\right] \qquad \ldots (28)$$

$$\Delta C_{m-GE} = C_m - C_{m-OGE} - C_{m\alpha}\left(\alpha-\alpha_{OGE}\right) + \\ - C_{m\delta s}\left(\delta_s - \delta_{s-OGE}\right) \qquad \ldots (29)$$

C_L, C_D and C_m represent aerodynamic coefficients estimated from flight data of a landing manoeuvre, whereas α and δ_s are the related flight measurements of angle of attack and stabilator deflection. $C_{L\text{-}OGE}$, $C_{D\text{-}OGE}$, $C_{m\text{-}OGE}$ are mean values of the aerodynamic coefficients computed providing flight data measurements gathered during the initial part of the landing approach (when the vehicle is out of GE) in input to the OGE aerodynamic model. Finally α_{OGE} and $\delta_{S\text{-}OGE}$ are mean values of angle-of-attack and stabilator deflection evaluated in the landing manoeuvre out of GE. The terms multiplying aerodynamic derivatives are introduced to correct the effects of flight condition changes during the manoeuvre (for the sake of brevity the derivatives in Equations (27) – (29) represent both contribution, with and without flap deflection). This approach assumes that the aerodynamic derivatives with respect to control surface and angle of attack are not functions of ground effect. An a posteriori correlation analysis between ground effect variations and α and δ_S can confirm or refute this hypothesis.

The obtained variations are used to identify the ground effect model described by Equation (9). First, for each flight test and for each aerodynamic coefficient the values of h_{GE} and of the maximum variation ΔC_{max} are computed. In order to evaluate h_{GE}, the standard deviation of the aerodynamic coefficient variation (denoted as $\sigma_{\Delta C}$) is calculated out of ground effect, during the initial part of the landing. Then h_{GE} is determined as the height above ground level (normalised with respect to the wing span) below which the absolute value of the coefficient variation becomes definitively greater than $\sigma_{\Delta C}$. ΔC_{max} is easily obtained by measuring the coefficient variation in $h = 0$.

Next, for each coefficient, the mean values (among all the examined flight tests) of h_{GE} and ΔC_{max} are computed. Finally, we consider the plane (h/b, ΔC) and compute in this plane the parable which satisfies the following conditions:

- it passes through the points $P_1 \equiv (0, \Delta C_{max})$ and $P_2 \equiv (h_{GE}, 0)$;
- it has null tangent in P_2.

For the assumptions made on the ground effect model, the coefficients of such parable coincide with the unknown parameters to be estimated, which are a_i, b_i and c_i of Equation (9).

6.0 RESULTS AND DISCUSSION

Before performing parameters estimation, a compatibility check was applied to flight data, in order to verify their consistency. Six manoeuvres (three for each configuration, with and without flap) were analysed to evaluate aerodynamic derivatives out of ground effect. For each configuration, estimation were performed on flight

https://doi.org/10.1017/S0001924000003833 Published online by Cambridge University Press

Table 1
Estimated aerodynamic derivatives

	Hybrid estimation		MATLAB estimation	
	No Flap	Flap	No Flap	Flap
C_{L0}	0·34 (0·06%)	0·72 (0·04%)	0·35	0·69
$C_{L\alpha}$	4·56 (0·07%)	4·57 (0·27%)	4·22	4·94
$C_{L\dot{\alpha}}$	0·12 (20·3%)	0 (-)	1·44	1·20
C_{Lq}	2·20 (1·34%)	4·00 (0·91%)	1·98	2·54
$C_{L\delta s}$	0·36 (0·13%)	0·53 (0·41%)	0·48	0·59
C_{D0}	0·029 (0·1%)	0·07(0·07%)	0·032	0·053
K_D	0.06 (0·12%)	0·05 (0·16%)	0·055	0·052
C_{m0}	–0·03 (0·3%)	–0·03 (0·5%)	–0·047	–0·013
X_{NP}	0·41 (0·09%)	0·34 (0·38%)	0·47	0·47

Table 2
TIC values for validation manoeuvres

	No Flap	Flap
α	0·11	0·07
q	0·13	0·11
TAS	0·02	0·02
θ	0·19	0·16

data of two manoeuvres, while the third one was used to validate the identified model prediction capability. Results are presented in Tables 1 to 2 and in Fig. 6.

Estimated aerodynamic derivatives are shown in Table 1. Columns 2 and 3 present the results of the proposed hybrid methodology for the two examined configurations. The Cramer-Rao bounds (in percentage) are reported in parentheses. This statistical indicator is an optimistic one and it must be multiplied for a fudge factor of typical 5-10 to obtain reliable values of estimation's standard deviation[2,12].

In order to validate the results, estimation was carried out using MATLAB's system identification toolbox, too. This toolbox contains several functions for parametric linear model estimation. The aircraft longitudinal linearised equations of motion were coupled with an output error method to identify the aircraft longitudinal characteristic. MATLAB estimations are presented in columns 4 and 5. They are in good agreement with values provided by the proposed hybrid technique, except for $C_{L\dot{\alpha}}$. The discrepancy in results for $C_{L\dot{\alpha}}$ is due to the absence of specific flight manoeuvres oriented to the estimation of this derivative. In fact in a conventional longitudinal manoeuvre, such as elevator doublet or 3-2-1-1, the pitch rate q is highly correlated to $\dot{\alpha}$, and the related derivatives are linearly dependent[2]. Therefore, without performing special manoeuvres, it is very difficult to distinguish the contribution to the global aerodynamic coefficient due to q from the one due to $\dot{\alpha}$.

In Fig. 6 the flight measurements of a validation manoeuvre are compared with the outputs of the identified simulation model, for configuration without flap deflection. All fittings are good, in particular short period dynamics are reproduced almost exactly. When flaps are deflected, MATLAB estimated model doesn't provide a good fitting for Phugoid dynamics, whereas hybrid estimated model matching of flight measurements is better. For both validation manoeuvres a light turbulence is present soon after 10 seconds. The inputs (stabilator deflection and thrust) are also reported in the figure.

In order to evaluate the overall goodness of fit, the Theil's Inequality Coefficient (TIC) is calculated for each of the output variables and for each manoeuvre. It is defined as[2]:

$$TIC = \frac{\sqrt{1/N \sum_{k=1}^{N} \left[\mathbf{z}(t_k) - \mathbf{y}(t_k)\right]^2}}{\sqrt{1/N \sum_{k=1}^{N} \left[\mathbf{z}(t_k)\right]^2} + \sqrt{1/N \sum_{k=1}^{N} \left[\mathbf{y}(t_k)\right]^2}} \quad \ldots (30)$$

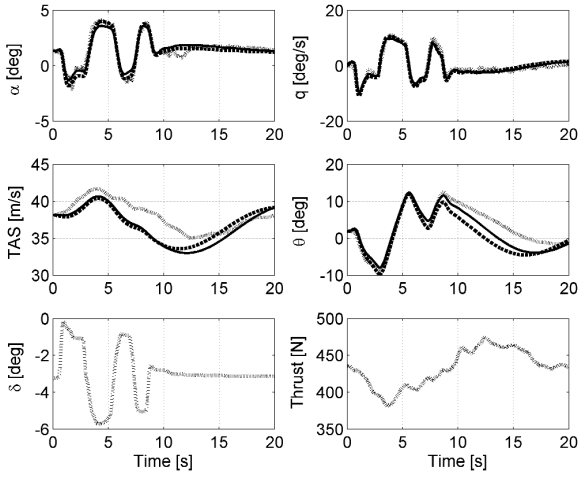


Figure 6. System outputs measured (dotted), simulated with hybrid (solid) and MATLAB (dashed) estimated models.

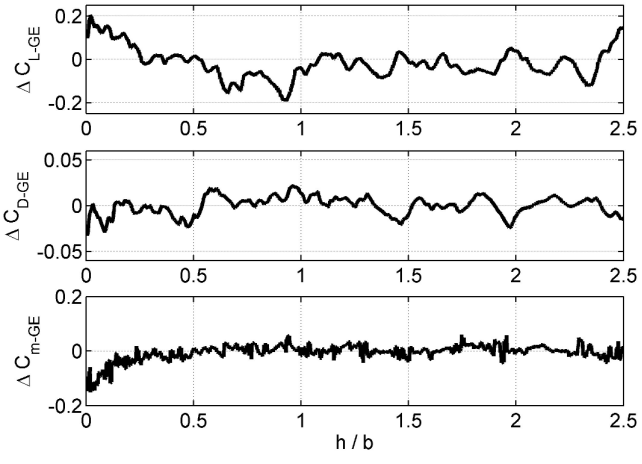


Figure 7. Variations of the aerodynamic coefficients due to ground effect (landing 1).

TIC = 0 means perfect fit, while *TIC* = 1 corresponds to the case of maximum inequality. In general *TIC* < 0·25 indicates a good agreement. *TIC* values for simulation using aerodynamic model estimated by means of the hybrid methodology are presented in Table 2. They confirm goodness of fitting.

Data gathered during 35 landings were examined to evaluate ground effect. Seven landings were considered good for estimation, the others were discarded due to the presence of atmospheric disturbances. It is worthy to note that identification manoeuvres were not performed during this critical phase of the flight.

In Figs 7 and 8 the variations of the aerodynamic coefficients due to ground effect, computed by means of Equations (27)-(29), are presented for two of the examined landings. For the sake of clearness only the last part of flight is shown. For what concerns the pitching moment variation, all the examined flight tests yielded the same trends and about the same magnitudes. As shown in the figures, the pitching moment coefficient quickly decreases when h/b becomes smaller than 0·3. It means that ground effect starts at h_{GE} = 0·3, corresponding to about 2·88 meters above ground level (being the wing span, used as non-dimensionalising factor, b = 9·6 meters). The variations of lift and drag coefficients haven't the same magnitudes in all the examined landings. In most of the analysed flight tests, lift coefficient increases in ground effect whereas drag coefficient decreases. However in few landings ground effect seems negli-

https://doi.org/10.1017/S0001924000003833 Published online by Cambridge University Press

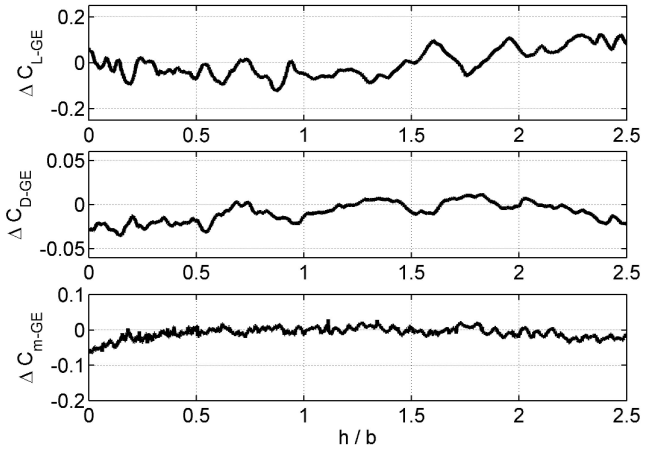


Figure 8. Variations of the aerodynamic coefficients due to ground effect (landing 2).

Table 3
Estimated ground effect parameters

Coefficient	h_{GE}	ΔC_{max}	a_i	b_i	c_i
C_L	0·3	+0·1	1·11	–0·667	0·100
C_D	0·3	–0·02	–0·222	0·133	–0·020
C_m	0·3	–0·05	–0·667	0·400	–0·060

gible at least on one of the two aerodynamic force coefficients. This behaviour is shown in Fig. 7 and Fig. 8. In fact, lift variation is evident in Fig. 7, where drag variation is small. On the other hand, Fig. 8 enhances the drag reduction, while small variation of lift is present. These results can be due to atmospheric disturbances experienced in flight or to other features which were not accounted for in the analysis. However, it is worthy to note that lift and drag variations are consistent for all the examined flight tests, that is, lift never decreases in ground effect, neither drag increases. In order to generalise the results and to identify the ground effect model, the value of h_{GE} estimated for pitching moment is assumed valid for lift and drag, too. Moreover the coefficients a_i, b_i and c_i related to lift and drag are evaluated as average values of the estimates computed for the seven analysed landings.

The estimates of a_i, b_i and c_i for all the longitudinal aerodynamic coefficients are reported in Table 3.

The identified aerodynamic model was validated in simulation. The simulation model is based on the six degrees of freedom rigid body equations of motion[12]. It includes the estimated aerodynamics and the flight control system used in flight.

A preliminary evaluation of the GE characteristics was obtained comparing two simulated landings, the first one was performed with the estimated ground effect model, the second one without ground effect. The effect of ground proximity (simulated by the first model) is evident when the altitude above ground level becomes lower than 2 metres. The results are shown in Fig. 9. The ground effect reduces the effectiveness of the stabilator. In fact a bigger deflection of stabilator produces smaller variations of angles of attack and pitch. The smaller angle of attack reduces the lift acting on the vehicle and consequently the touchdown point is anticipated.

The outputs of the simulation model, inclusive of the ground effect, were also compared with flight measurements (acquired in a test that wasn't used for estimation). The results are shown in Fig. 10. With the aim to perform the comparison between simulated and experimental data both simulation and flight test were performed with low turbulence level. The simulator uses the von Karman model to model the atmospheric turbulence disturbances. The matching is very good for angle of attack and pitch angle. Simulated stabilator deflection has the same behaviour of flight measurement, except for

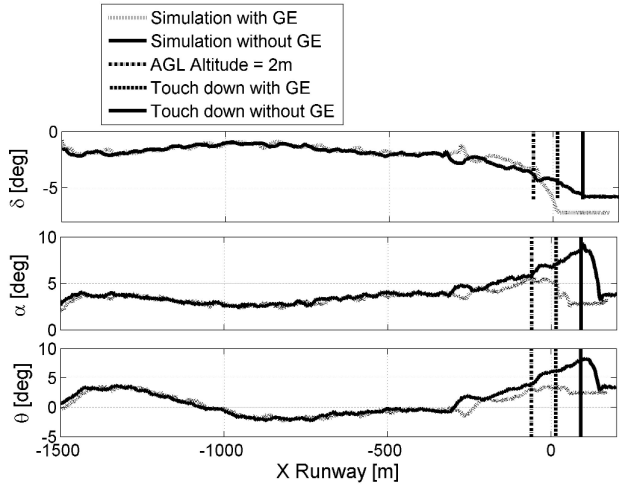


Figure 9. Comparison between simulation with and without ground effect; the height above ground level where ground effect becomes evident (2m) and the simulated touchdown points are also shown in the figure.

a small off-set. Also simulated and experimental touchdown points are in practice coincident. Ground effect is evident when height above ground level becomes lower than about two metres, as indicated in the figure. In fact, the increase of stabilator deflection (in absolute value) in the last part of the trajectory, while pitch angle remains about constant, confirms that the ground effect is present.

The estimated aerodynamic model, used in simulation, is able to exactly reproduce this behaviour.

After these validation, the identified aerodynamic model, inclusive of the ground effect, was used to design the flight control system that successfully performed many autonomous landings[13].

7.0 CONCLUSION

A hybrid multi-step frequency and time domains technique for longitudinal aerodynamic model identification is described in the paper. The main advantage of the proposed method is that it gives reliable results also in the dynamic phases of the flight (i.e. landing) or even when no dedicated identification manoeuvres are executed.

The application of the method to the flight data of an ultra light experimental aircraft allows to get the following main findings:

(*i*) The technique properly identifies the longitudinal aerodynamic model out of ground effect, using flight data gathered during identification manoeuvres. The validation of the estimated model enhanced that the identification results are comparable and in some cases better than the ones obtained by means of MATLAB's system identification toolbox.

(*ii*) The application of the technique to flight data of landing manoeuvres allows to identify the ground effect too, evaluating and modelling the variations of longitudinal aerodynamic coefficients acting on the vehicle when it is in ground proximity. It is worthy to note that identification manoeuvres are not performed to identify the ground effect model.

(*iii*) The validation of the ground effect model is carried out using flight data and simulation model and confirms the reliability of the identified model.

The estimated longitudinal aerodynamic model, inclusive of the ground effect, was used to design the flight control system that successfully performed many autonomous landings.

https://doi.org/10.1017/S0001924000003833 Published online by Cambridge University Press

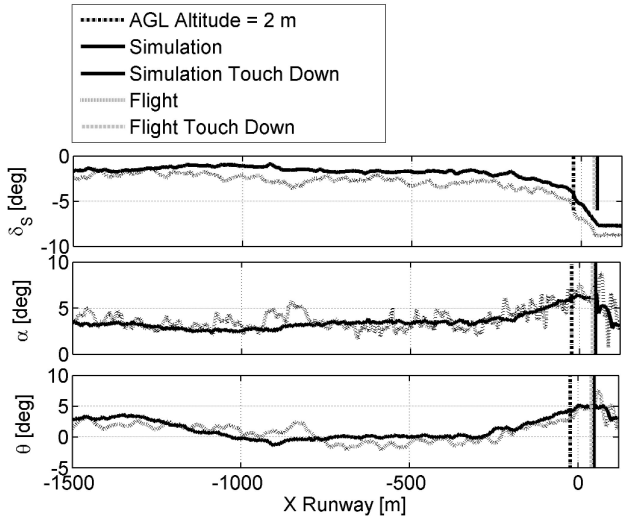


Figure 10. Comparison between flight measurements and simulation outputs; the height above ground level where ground effect becomes evident (2m) and the measured and simulated touchdown points are also shown in the figure.

REFERENCES

1. MORELLI, E.A. Real-time parameter estimation in the frequency domain, *J Guidance, Control and Dynamic*, September–October 2000, **23**, (5), pp 812-818.
2. JATEGAONKAR, R.V. Flight vehicle system identification: A time domain methodology, *AIAA Progress in Aeronautics and Astronautics*, 2006, **216**, AIAA, Reston, VA, USA.
3. CURRY, R.E. Dynamic ground effect for a cranked arrow wing airplane, 1997, NASA Technical Memorandum 4799, Edwards, CA, USA.
4. CORDA, S., STEPHENSON, M.T., BURCHAM, F.W and CURRY, R.E. Dynamic ground effects flight test of an F-15 aircraft, 1994, NASA Technical Memorandum 4604, Edwards, CA, USA.
5. DEVESA, B., JOURDAN, C. and MARC, C. Ground-effect identification and autoland system validation from flight data, *J Aircr*, July–August 2004, **41**, (4), pp 730-734.
6. ROHLF, D. Global model approach for X-31 VECTOR system identification, *J Aircr*, January–February 2005, **42**, (1), pp 54-62.
7. EMSLIE, K., GARNER, H.C., JUPP, J.A. and WEDDERSPOON, J.R. Low-speed longitudinal aerodynamic characteristics of aircraft in ground effect, 1972, ESDU No 72023.
8. AHMED, M.R., TAKASAKI T and KOHAMA, Y. Aerodynamics of a NACA4412 airfoil in ground effect, *AIAA J*, January 2007, **45**, (1), pp 37-47.
9. LEE, P.H., LAN, C.E. and MUIRHEADT, V.U. Experimental investigation of dynamic ground effect, *J Aircr*, June 1989, **26**, (6), pp 497-498.
10. HOFF, J.C. and COOK, M.V. Aircraft parameter identification using an estimation-before-modelling technique, *Aeronaut J*, August-September 1996, **100**, (997), pp 259-268.
11. VITALE, A., CORRARO, F., BERNARD, M. and DE MATTEIS, G. Unscented Kalman filtering for reentry vehicle identification in the transonic regime, *J Aircr*, September-October 2009, **46**, (5), pp 164-1659.
12. MAINE, R.E and ILIFF, K.W. Application of parameter estimation to aircraft stability and control, June 1986, NASA Reference Publication 1168.
13. DI VITO, V., DE LELLIS, E., CORRARO, F., GENITO, N., MARRONE, C. and CINIGLIO, U. UAV free path safe DGPS/AHRS autolanding: Algorithm and flight tests, June 2008, UAV SYSTEM 2008 — International Technical Conference & Exhibition, Paris, France.
14. MCCORMIC, B.W. *Aerodynamics, aeronautics and flight mechanics*, 1995, John Wiley and Sons, New York, USA.

https://doi.org/10.1017/S0001924000003833 Published online by Cambridge University Press